European Polymer Journal 255 (2026) 114886

Contents lists available at ScienceDirect

European Polymer Journal

journal homepage: www.elsevier.com/locate/europolj

Solvent effects in the enzymatic synthesis of poly(glycerol adipate): A design of experiments approach toward sustainable media

Gabriel F.S. Brito [a,b], Emily G. Dixon [a], Mei Y. Young [a], Adam J. Lee [d], Daniel M. Day [d], Amy R. Goddard [d], Fabricio Machado [b,c], Philippa L. Jacob [a,*], Vincenzo Taresco [a,*]

[a] School of Chemistry, University of Nottingham, University Park, Nottingham NG7 2RD, UK
[b] University of Brasília, Institute of Chemistry, Campus Universitário Darcy Ribeiro, Brasília, DF, Brazil
[c] Chemical Engineering Graduate Program, Federal University of Goiás, Campus Samambaia, Goiânia 74690-900, GO, Brazil
[d] Croda Europe Ltd, Foundry Lane, Ditton, Widnes, UK

ARTICLE INFO

Keywords:
Poly(glycerol adipate)
Enzymatic polycondensation
Design of experiments
Sustainable solvents

ABSTRACT

The identification of sustainable reaction media remains a central challenge in enzymatic polymer synthesis, where solvent properties strongly influence enzyme activity, polymer chain growth, and overall process sustainability. Here, a Design of Experiments (DoE) strategy was employed to systematically investigate the enzymatic synthesis of poly(glycerol adipate) (PGA) using *Candida antarctica* lipase B (*Ca*LB) across alternative solvent systems. The influence of solvent (2-methyltetrahydrofuran (2-MeTHF), methyl ethyl ketone (MEK), cyclopentyl methyl ether (CPME), and supercritical carbon dioxide ($scCO_2$)), temperature, enzyme loading and reaction time were simultaneously evaluated in the polycondensation of two adipate-based systems – divinyl adipate (DVA) and adipic acid (AA) with glycerol. Across the experimental design space, conversions ranged from 9 to 100 % for DVA and 0–96 % for AA, while the resulting polymers spanned a broad structural range with weight-average molar masses reaching 16300 g/mol and 36700 g/mol for DVA and AA, respectively. Contour plot modelling revealed clear solvent-dependent behaviour, with 2-MeTHF consistently supporting efficient polymerisation, whereas MEK and CPME displayed intermediate performance, and $scCO_2$ exhibited limitations associated with solubility and mass-transfer constraints. The DoE framework enabled the mathematical modelling of solvent effects, providing a predictive strategy for exploring sustainable reaction media while minimizing experimental effort. The results demonstrate how statistically guided experimentation can accelerate the identification of greener reaction media for enzymatic polyester synthesis while enabling rational control over polymer structure.

1. Introduction

In the landscape of sustainability and biodegradability, aliphatic polyesters occupy a particularly important position in many industrial areas [1–3]. Traditionally, these materials are synthesized through step-growth or chain-growth polymerisations catalysed by metal-based systems and conducted at elevated temperatures [4–6]. While effective, such approaches often suffer from limited control over polymer architecture, potential contamination by residual metals, and energy-intensive processing conditions. Enzymatic polymerisation has emerged as an attractive alternative to conventional routes [7]. Lipase-catalysed polyester synthesis offers several advantages, including mild reaction conditions, high chemo- and regioselectivity, reduced toxicity, and compatibility with renewable monomers [8,9]. Enzymatic polycondensation in particular has proven effective for producing functional aliphatic polyesters [10–12]. Within this context, poly(glycerol adipate) (PGA) has attracted considerable attention as a biodegradable and biocompatible polyester platform [11,13]. A defining structural feature of PGA is the presence of pendant secondary hydroxy groups along the backbone. These groups impart amphiphilicity, enable post-polymerisation functionalization, and promote self-assembly into nanoparticles in water, making PGA attractive for biomedical applications [11,12,14–18]. These secondary hydroxy groups are retained during enzymatic polymerisation, in contrast to Flory's classical polycondensation theory which assumes equal reactivity of functional groups [19]. In conventional polycondensations these hydroxy groups

* Corresponding authors.
E-mail addresses: pippy.jacob@nottingham.ac.uk (P.L. Jacob), vincenzo.taresco@nottingham.ac.uk (V. Taresco).

https://doi.org/10.1016/j.eurpolymj.2026.114886
Received 16 April 2026; Received in revised form 9 June 2026; Accepted 10 June 2026
Available online 12 June 2026

are often consumed in other leading to more branched or crosslinked structures [11,20,21]. The nature of the adipate derivative used in the polymerisation plays a decisive role in determining the efficiency of the polymerisation, the molar mass, and structural characteristics of the resulting polymer [11,22].

Among the most common monomers, AA [10] and DVA [11,22] have been successfully used (Scheme 1). When AA is used as the acyl counterpart, esterification occurs via a condensation mechanism that generates water as a by-product [10,23]. Since the presence of water results in an equilibrium state for the polyesterification, continuous by-product removal, typically through the use of molecular sieves, high temperature or reduced pressure, are required to achieve appreciable degrees of polymerisation [22]. By contrast, during DVA transesterification, the vinyl alcohol by-product spontaneously tautomerizes to acetaldehyde, which is volatile and readily removed from the system. On a large scale, however, acetaldehyde can be less straightforward to handle than water, introducing additional considerations in reaction setup and safety. This irreversible removal of the side-product drives the reaction equilibrium toward polymer formation, leading to higher conversions and resulting polymer under relatively mild reaction conditions (50 °C) in THF and 2-MeTHF as solvents [11,22]. Overall, while both adipate derivatives enable the enzymatic formation of hydroxylated polyesters, DVA can be considered a model monomer, offering faster reaction kinetics, and providing better structural control [10,11,13,22]. The degree of glycerol substitution, chain branching, molar mass, and dispersity are all governed by a delicate balance between enzyme selectivity, reaction kinetics, substrate solubility, and removal of condensation by-products.

Parameters such as reaction temperature have been shown to strongly influence enzyme conformation and regioselectivity, directly affecting the degree of branching and the apparent molar mass of the resulting polymer. To date, most investigations into PGA synthesis have relied on one-factor-at-a-time optimization strategies, typically focusing on temperature, reaction time, or monomer feed ratio independently. These approaches inherently fail to capture interactions between reaction variables, which are expected to be particularly significant in enzymatic polymerisations.

More recently, a greener alternative, 2-MeTHF, has been explored as a replacement for THF [15]. 2-MeTHF effectively replaced THF without compromising enzyme activity or polymer formation, while offering advantages in terms of solvent sustainability. However, this assessment was conducted by varying the reaction medium as a single factor. Given these considerations, a multivariate and statistically rigorous approach is required to disentangle the relative importance of individual parameters and their interactions. DoE provides a powerful framework to achieve this goal, enabling simultaneous variation of multiple factors while minimizing experimental effort. By quantifying both main effects and interaction terms, DoE facilitates a mechanistic understanding of how processing conditions govern polymerisation outcomes, rather than relying on empirical optimization [24,25].

In this work, a multifactorial DoE is employed to systematically evaluate the effects of key process parameters on polymer formation and quality during the enzymatic synthesis of PGA using glycerol and either using AA or DVA. The effects of (i) solvent (2-MeTHF; MEK; CPME; $scCO_2$), (ii) temperature, (iii) reaction time, and (iv) enzyme loading are assessed in parallel, using monomer conversion, weight-average molar mass (M_w), dispersity ($Đ$), and the extent of glycerol 1,2,3-trisubstitution and 1,2-disubstitution as quantitative responses. The investigated parameter ranges were defined according to the intrinsic reactivity of each adipate derivative, with reaction time and enzyme loading adjusted when required to ensure comparable and meaningful evaluation across systems. By correlating these outputs with controlled variations in reaction conditions, this study aims to establish a robust

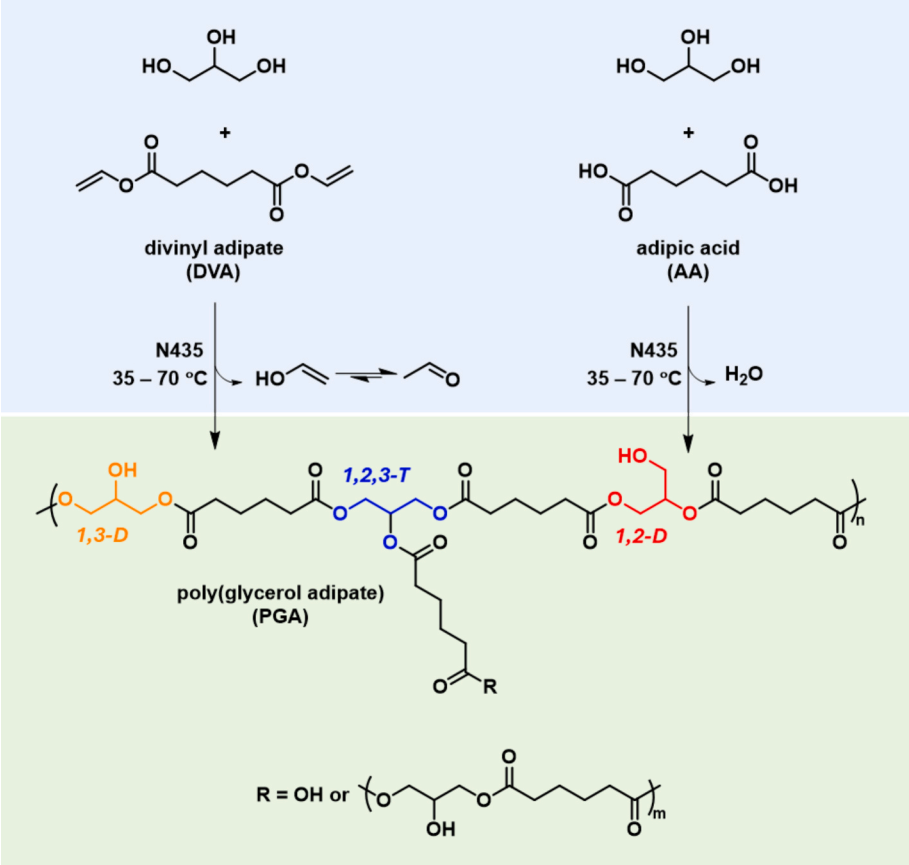

Scheme 1. Reaction scheme demonstrating two different adipate-based monomers and their respective by-products to produce PGA via enzymatic polycondensation. 1,2-Disubstitution, 1,3-disubstitution and 1,2,3-trisubstitution of glycerol are shown in red, orange and blue.

structure–process–property relationship for PGA synthesis, providing fundamental insights into enzymatic polycondensation and practical guidelines for the reproducible synthesis of PGA with tailored architectures.

2. Materials and methods

2.1. Materials

Sustine® 110 IM (also known as Novozym 435 lipase), derived from *C. antarctica* (>5000 U/g) and immobilized on an acrylic microporous resin was kindly donated by Novonesis. Glycerol, adipic acid (AA), 2-methyltetrahydrofuran (2-MeTHF), and molecular sieves 3Å were purchased from Sigma-Aldrich, UK. Divinyl adipate (DVA) [4074–90–2] was purchased from ABCR, UK. Methyl ethyl ketone (MEK) was purchased from Sigma-Aldrich, UK, and cyclopentyl methyl ether (CPME) from Thermo Scientific, UK [5614–37–9]. Carbon Dioxide (CO_2, SCF grade 5.5, 99.9995 %) was obtained from Air Products and Chemicals Inc. All chemicals were used as received, and solvents were used without further purification unless otherwise stated. Solvent evaporation was performed using a rotary evaporator under reduced pressure.

2.2. PGA synthesis

In a typical procedure, glycerol (5 mmol) and DVA (5 mmol) were poured into a 20 mL glass vial and dissolved in 5 mL of the selected solvent. The resulting mixture was stirred at 200 rpm with a magnetic stirrer and then heated. To this, lipase was added and then the reaction time started. A needle was inserted through the rubber septum to facilitate the release of acetaldehyde. The reaction was stopped by removing the immobilized enzyme by filtration, followed by evaporation of the solvent under reduced pressure. The product was stored at −20 °C to minimize possible hydrolysis side reactions [15].

In reactions employing AA, freshly activated molecular sieves (1.8 g) were added to the reaction to trap the water produced during esterification. This amount corresponds to twice the adsorption capacity (20 wt %) required to retain all the water expected for complete conversion of the diacid [23].

For reactions performed in $scCO_2$, all reactions were performed in a high-pressure autoclave. The stirrer rate was kept constant at 200 rpm and a basket containing enzyme and molecular sieves (for AA reactions) was attached to the stirrer shaft (Supporting Information – Section 1, Fig. S1). The reagents were placed inside the autoclave, which was then sealed. The autoclave was heated to 31 °C and pressured to 83 bar (above the critical point of CO_2) then the reaction was further heated and pressurised to the respective reaction temperature and pressure. For the reactions screened, the temperature was varied between 35 and 70 °C, while the pressure was fixed at 200 bar which has been previously shown to be optimal for enzymatic polycondensation reactions [26–30].

2.3. ^1H NMR analysis

Approximately 10 mg of sample was dissolved in 0.75 mL of acetone-d_6 or deuterated dimethyl sulfoxide (DMSO-d_6) and analysed using a Bruker Avance 400 MHz spectrometer operating at 400 MHz, assigning chemical shifts in parts per million (ppm). MestReNova 15.0.0 copyright 2023 (Mestrelab Research S. L.) was used to analyse the spectra. Two drops of deuterium oxide (D_2O) were added to the samples prepared with DMSO-d_6.

Conversion is reported as the total amount of monomer consumed (%) and is calculated as per Equations S1, when using acetone-d_6, and Equation S2 when using DMSO-d_6.

The degree of glycerol substitution was determined by ^1H NMR spectroscopy, allowing the quantification of disubstituted (1,2-D) and trisubstituted (1,2,3-T) glycerol units [11,15]. For polymers obtained using DVA, the integral of the methylene signal of the adipate repeating unit at 2.36 ppm was used as internal reference and normalized to four protons. The molar percentage of trisubstituted glycerol was obtained from the ratio between the normalized signal and the integral of the glycerol proton at 5.28 ppm, assigned to the fully substituted glycerol environment. The molar percentage of disubstituted glycerol was determined analogously using the glycerol proton signal at 5.08 ppm, corresponding to disubstituted glycerol units.

For polymers synthesized from AA, the same normalization procedure was applied. The methylene signal of the adipate unit at 2.29 ppm was integrated and normalized to four protons to serve as internal reference. The molar percentage of trisubstituted glycerol was calculated using the ratio between the normalized adipate signal and the glycerol proton at 5.16 ppm, attributed to trisubstituted glycerol units. The molar percentage of disubstituted glycerol was determined from the glycerol proton signal at 4.92 ppm, assigned to the disubstituted glycerol environment.

2.4. Gel permeation chromatography (GPC)

GPC was performed in THF (HPLC grade, Fisher Scientific) as the eluent at 40 °C using two Agilent PL-gel mixed-D columns and two Agilent PL-gel mixed-E columns in series, an injection loop of 50 µL, with a flow rate of 1 mL/min. A differential refractometer was used for the detection of samples (solution containing approximately 4 mg dissolved in 2 mL of THF, filtered in 0.22 µm Teflon filter). The system was calibrated using poly(methyl methacrylate) standards with average molar mass in the range from 540 to $1.02x10^6$ g/mol and dispersity ($Đ$) close to 1.0.

2.5. Experimental design

Given the strong interdependence of solvent effects, enzyme loading, temperature, and reaction time, a DoE was implemented to systematically evaluate how these parameters collectively influence polymerisation performance [24]. The experimental grid was generated based on a D-Optimal design using MODDE Pro® 13.1 software (Sartorius). This generated an experimental plan of 25 experiments for each adipate derivative, using the factors, natural levels and responses, as presented in Table 1. The table of experiments for the DVA and AA reactions are presented in Supporting Information – Section 1, Table S1 and Table S2, respectively. The influence of enzyme loading (1, 3 and 6 wt%) relative to the total monomer content, reaction temperature (35, 50, and 70 °C), and reaction time (3, 5, and 7 h) was investigated according to the experimental design for the DVA reactions. For the AA reactions, the experimental design investigated the same factors, but with increased enzyme loadings (3, 7 and 14 wt%) and reaction times (6, 18 and 24 h), in agreement with literature values [23,31,32]. The possibility of reaching an equilibrium state, due to the presence of water combined with the fact that water is a poorer leaving group, than acetaldehyde likely contribute to the higher enzyme loadings reported when using AA compared to DVA. Furthermore, work by Saller *at al.* suggest that the acid environment of AA in solution has a deactivating effect on lipase

Table 1
Design of experiments parameters for the syntheses of PGA using DVA and AA as an adipate counterpart.

Factor	DVA – Levels	AA – Levels	Responses
Enzyme loading (%)	1, 3 and 5	3, 7 and 14	M_w[a]
Temperature (°C)	35, 50 and 70	35, 50 and 70	Dispersity ($Đ$)[a]
Time (h)	3, 5 and 7	6, 18 and 24	Conversion[b]
Solvent	2-MeTHF, MEK, CPME and $scCO_2$	2-MeTHF, MEK, CPME and $scCO_2$	1,2-D and 1,2,3-T

[a] Determined by GPC, calibrated against PMMA standards.
[b] Defined as monomer consumption.

enzymes, resulting in higher enzyme loadings for these reactions [33]. The reaction temperatures investigated remained comparable to those of the DVA reactions (35, 50 and 70 °C). Both DoEs evaluated alternative solvent systems with improved safety and sustainability profiles, including 2-MeTHF, MEK, CPME and $scCO_2$ [34–38].

3. Results and Discussion

Reaction medium plays a critical role in enzymatic polymerisation, as solvent properties directly influence enzyme activity and polymerisation kinetics through their effects on substrate solubility, and the microenvironment surrounding the immobilized catalyst. Parameters such as polarity, hydrophobicity, hydrogen-bonding capacity, and the protic or aprotic nature of a solvent can significantly influence conversion, attainable molar mass and overall reaction rates [39,40]. As a result, even subtle differences in solvent physicochemical characteristics may lead to substantial changes in polymer growth behaviour and final material properties.

In this context, the selection of alternative and potentially greener solvents becomes particularly relevant, not only to improve environmental sustainability but also to understand how such solvents may tune enzymatic performance and polymerisation outcomes [41]. Although conventional media such as tetrahydrofuran have been widely employed in PGA synthesis, increasing emphasis on safer and more sustainable processes has motivated the search for viable substitutes [42,43]. Bio-derived ethers such as 2-MeTHF and CPME, industrially relevant ketones such as MEK, and non-conventional reaction media such as $scCO_2$ provide distinct solvation environments that may markedly influence enzyme stability, mass transfer, and polymer chain growth. However, their effects on PGA formation have not been systematically compared, and comprehensive evaluations across different solvent classes remain scarce.

3.1. DoE applied to DVA screening

To quantitatively interpret trends associated with the polycondensation of DVA and glycerol, the dataset was modelled using multiple linear regression (MLR) implemented in the MODDE software, with conversion initially selected as the primary response variable. Extended coefficient models and tables containing the estimated MLR model parameters are provided in the Supporting Information – Section 2, Fig. S3 to Fig. S8 and Tables S3 to S8. The main text focuses on the interpretation of the response contour plots, which summarise the effects of the experimental factors on the measured responses. The general regression equation for MLR model is provided in the Supporting Information (Equation S3 and Equation S4) and can be used to derive individual predictive models for each response using the variables defined in the corresponding coefficient tables for each adipate derivative.

DVA reactions showed that near-quantitative conversion (determined by ^{1}H NMR, Supporting Information – Fig. S2A, Equation S1) could be achieved within the experimental domain, with values ranging from 9 % to 100 % (Fig. 1). There is, however, a pronounced dependence on the reaction medium. In both MEK and 2-MeTHF, conversions close to 100 % were observed over a broad range of temperature and enzyme loadings, even at shorter reaction times, indicating that these solvents provide favourable conditions for efficient polycondensation. In contrast, $scCO_2$ and CPME exhibit a pronounced dependence on temperature, time, and enzyme loading. At lower temperatures and shorter reaction times, conversion drops significantly, requiring simultaneous increases in these parameters to approach high monomer consumption. CPME displays intermediate behaviour, with moderate to high conversions achieved only when temperature, reaction time, and enzyme loading are simultaneously increased to approach quantitative conversion. The comparatively limited conversion observed in CPME and $scCO_2$ can be attributed to reduced solubility of glycerol and the growing polymer chain in these media. Restricted solvation likely impairs mass transfer and decreases effective contact between substrate and immobilized enzyme, thereby slowing the overall reaction rate.

These results indicate that, within most of the investigated domain, high conversion can be readily achieved, particularly in 2-MeTHF and MEK, where monomer consumption approaches completion across a broad range of conditions. In $scCO_2$ and CPME, there is a stronger dependence on harsh conditions, confirming that solvent effects play a central role in governing reaction efficiency. Once high conversion is achieved, further differentiation between experimental conditions shifts toward structural aspects of the resulting polymers, particularly the distribution of glycerol substitution patterns. In this context, the analysis of 1,2,3-T and 1,2–D provides deeper insight into how reaction parameters influence polymer structure.

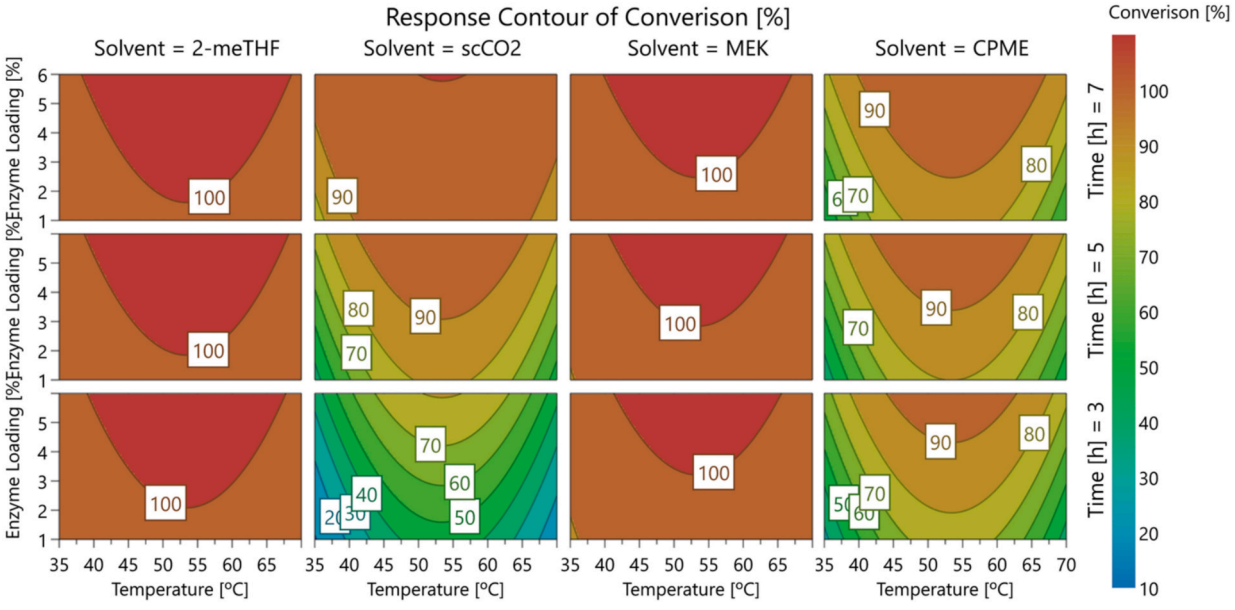

Fig. 1. Predicted conversion (%) contour plots for DVA reactions as a function of temperature and enzyme loading, presented for four solvents (2-MeTHF, $scCO_2$, MEK and CPME) at different reaction times (3, 5 and 7 h).

The contour plots for the 1,2,3-T response (Fig. 2A) show a clear increase with enzyme loading and temperature in 2-MeTHF and MEK, indicating that higher catalytic availability combined with elevated temperatures promotes the formation of more highly substituted glycerol units. Among the solvents evaluated, 2-MeTHF consistently provides the highest predicted 1,2,3-T values across the design space, whereas CPME and $scCO_2$ exhibit comparatively lower levels. In these latter media, the reduced 1,2,3-T response appears to be associated primarily with the lower overall conversion achieved under comparable conditions, rather than with a distinct change in substitution selectivity. Within the investigated reaction time range (3–7 h), reaction duration does not emerge as a dominant factor compared to enzyme loading and solvent effects, indicating that 1,2,3-T differentiation is primarily controlled by catalytic and medium-related parameters.

The contour plots for 1,2-D (Fig. 2B) indicate a monotonic increase in 1,2-D with temperature, enzyme loading, and reaction time. Similar response surfaces across solvents suggest that conditions associated with higher reactivity systematically increase secondary substitution, independent of the reaction medium.

Variations in glycerol substitution influence the architecture of the polymer backbone and, consequently, the formation of high molar mass species. Increased levels of 1,2,3-T modify chain connectivity and may alter the balance between linear growth and structural complexity. Therefore, analysis of M_w allows evaluation of how reaction parameters control the extent of polymerisation and the development of high-mass fractions.

The M_w varied substantially across the design space (200 to 16300 g/mol), revealing a strong sensitivity to both solvent and enzyme loading. The contour plots for M_w (Fig. 3) reveal a strong dependence of chain growth on the reaction medium. 2-MeTHF consistently provides the highest predicted values across the design space, with a pronounced increase at elevated enzyme loading and temperature indicating that this medium promotes the formation of high molar mass fractions. In contrast, $scCO_2$ exhibits comparatively low and weakly responsive M_w values throughout the experimental domain, suggesting restricted chain extension in this medium, in agreement with the conversion metrics.

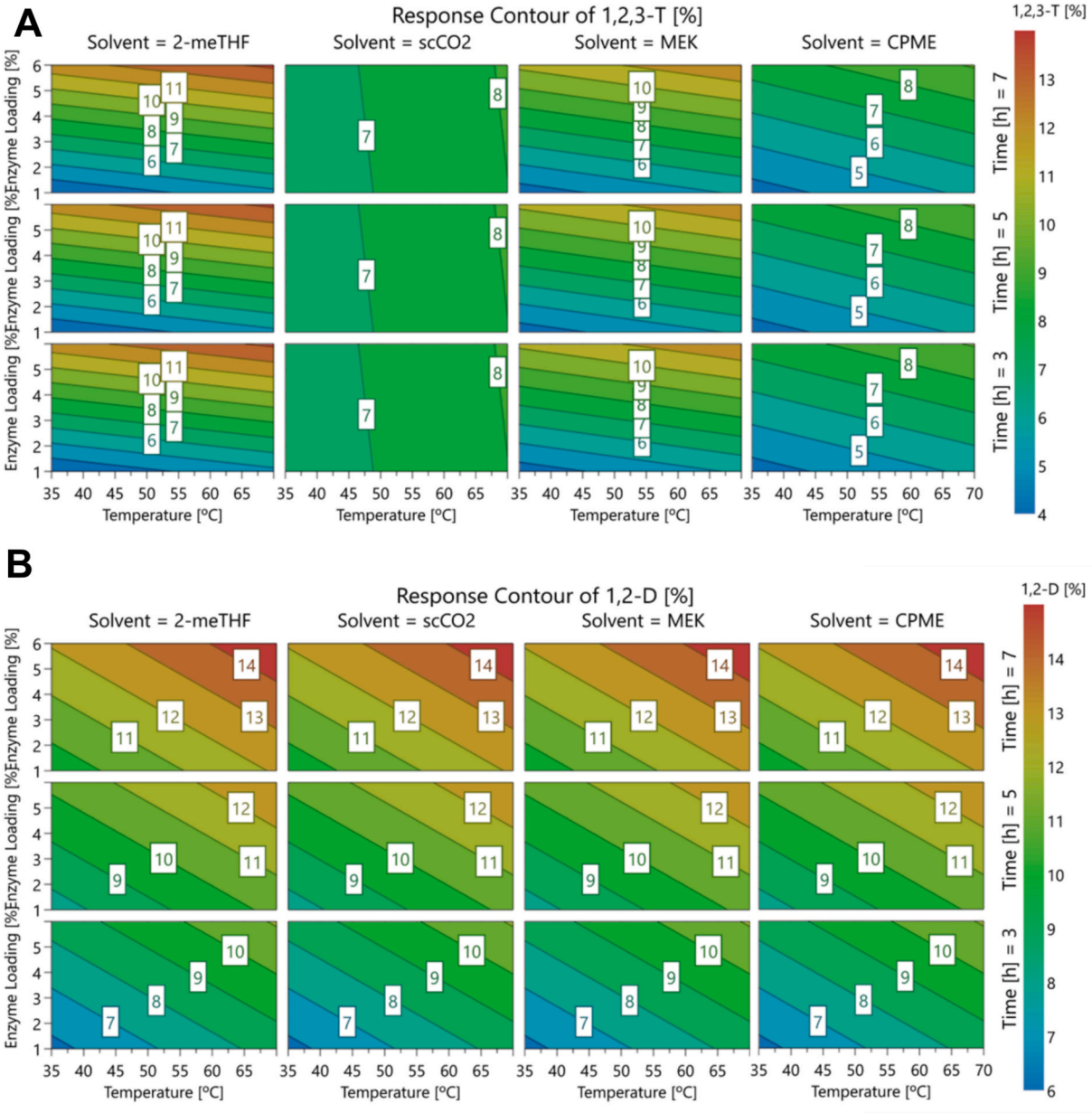

Fig. 2. Predicted (A) 1,2,3-Trisubstitution (%) and (B) 1,2-Disubstitution (%) contour plots for DVA reactions as a function of temperature and enzyme loading, presented for four solvents (2-MeTHF, $scCO_2$, MEK and CPME) at different reaction times (3, 5 and 7 h).

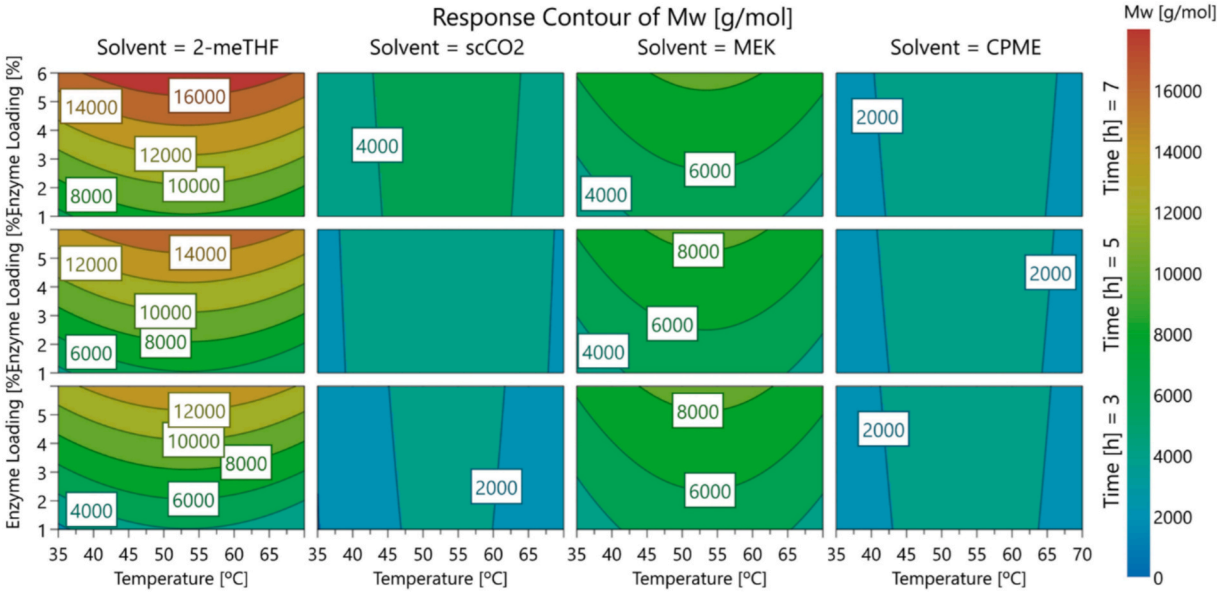

Fig. 3. Predicted M_w (g/mol) contour plots for DVA reactions as a function of temperature and enzyme loading, presented for four solvents (2-MeTHF, $scCO_2$, MEK and CPME) at different reaction times (3, 5 and 7 h).

MEK displays intermediate behaviour, with moderate M_w values that increase within a narrower temperature range, while CPME maintains relatively low molar masses with limited sensitivity to process variables. A complementary analysis of the number-average molar mass (M_n) is provided in the Supplementary Information – Section 2, Fig. S9.

Although high conversion is achieved across much of the experimental domain, M_w does not scale directly with monomer consumption, indicating that conversion alone does not determine the extent of the chain to grow but is also governed by solvent-mediated kinetic and diffusion effects. For example, reactions in MEK had high monomer conversion, however the M_w of the resulting polymers was comparable to that of $scCO_2$. It is important to emphasize that the molar mass values were obtained by GPC using polymethylmethacrylate standards for calibration (Section 2.4); therefore, they should be interpreted as relative indicators for comparative purposes rather than absolute values.

A qualitative correspondence is observed between M_w and 1,2,3-T, particularly in 2-MeTHF, where higher levels of 1,2,3-T coincide with increased apparent molar mass. It is worth noting that the PMMA standards used for GPC calibration are based on linear polymers. In the present case, however, the polymers are likely to become more branched as the 1,2,3-T increases. Consequently, the observed behaviour may be associated with differences in hydrodynamic volume between branched and linear polymers. In contrast, 1,2-D increases more uniformly across solvents and does not consistently translate into higher M_w values, suggesting that the increase in M_w is more strongly associated with solvent-dependent structural effects than with overall reactivity. Importantly, variations in M_w are accompanied by changes in $Đ$, indicating that conditions promoting higher molar mass also influence the breadth of the molar mass distribution.

The contour plots for $Đ$ (Fig. 4) show a consistent increase in dispersity values with increasing reaction factors across all solvent systems. Higher values are systematically observed at longer reaction times and

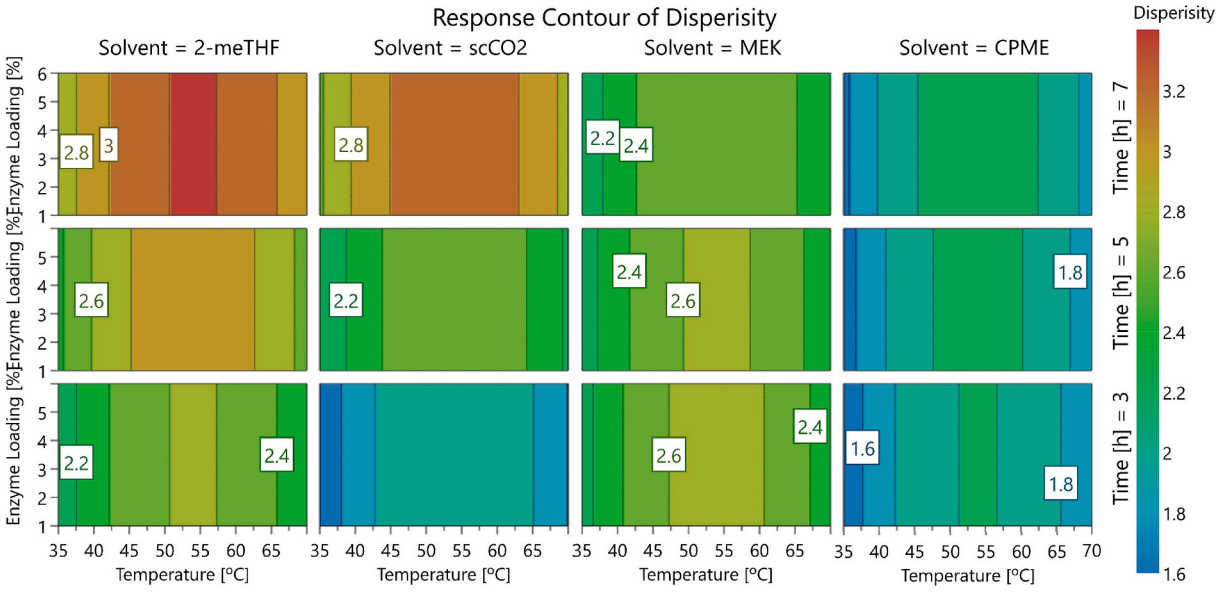

Fig. 4. Predicted Dispersity ($Đ$) contour plots for DVA reactions as a function of temperature and enzyme loading, presented for four solvents (2-MeTHF, $scCO_2$, MEK and CPME) at different reaction times (3, 5 and 7 h).

at increased temperature. Although enzyme loading trends are not strongly pronounced in the contour plots, experimental data indicate that enzyme concentration plays a relevant role in $Đ$, particularly in 2-MeTHF, as shown in Table S1.

Two experiments exhibited markedly elevated values, entries N7 and N17, with dispersity values of 4.9 and 6.5, respectively. Both runs were conducted in 2-MeTHF under the highest temperature and enzyme loading conditions, where rapid polymer chain extension, increased medium viscosity, and intensified transesterification or chain redistribution processes are expected. These combined effects likely broadened the molar mass distribution, resulting in higher dispersity. In addition, these samples presented the highest 1,2,3-T values under the experimental domain, with 12 and 16 %, for samples N7 and N17, respectively, which is consistent with the correlation previously observed between M_w and 1,2,3-T.

The removal of outliers, entries N7 and N17, to improve model performance may reduce the apparent magnitude of the enzyme loading effect in the fitted response surfaces, thereby shifting the model emphasis toward other factors. This shift in model behaviour is reflected in the fitted equation for 2-MeTHF, in which enzyme loading is not retained as a contributing variable, as can be seen in Equation (1). The independent variables were defined as X_1 (solvent), X_2 (enzyme loading), X_3 (temperature) and X_4 (reaction time), as detailed in the Supporting Information – Equation S3 and S4 and the regression coefficients are also presented in Table S7.

$$Đ = 2.54013 + 0.373912\,X_1 + 0.0789534\,X_3 + 0.220429\,X_4 - 0.474561\,X_3^2 \quad (1)$$

It is important to emphasize that the model presented in this work was selected based on superior goodness-of-fit metrics, and therefore most accurately reflects the behaviour of the experimental data within the investigated design space. Solvent-dependent differences remain evident in the $Đ$, with 2-MeTHF generally yielding higher values and CPME the lowest, while $scCO_2$ and MEK show intermediate behaviour. In many of the contour plots, $Đ$ values exceeding of 2 are observed, indicating the formation of branched polymers, deviating from ideal Flory behaviour associated with linear step growth polymers [19,44]. It is possible that the branching is the result of unequal functional group stoichiometry, or intermolecular transesterification.

It should be noted that, despite the low conversions obtained in $scCO_2$, higher enzyme levels led to higher dispersity, indicating that the molecular characteristics of the polymer formed are strongly influenced by enzyme loading under these conditions. Gameiro *et al.* showed that the enzymatic polycondensation of glycerol and succinic acid in $scCO_2$ using 25 wt% *Ca*LB to produce poly(glycerol succinate), demonstrating that the presence and loading of the enzyme play a key role in determining the molecular characteristics of the polymer formed under $scCO_2$ conditions [45].

3.2. DoE applied to AA screening

An analogous multifactorial design was conducted using AA in place of DVA. Given the intrinsic differences in reactivity between the two systems, the ranges of the investigated parameters were adjusted accordingly, particularly with respect to reaction time and enzyme loading, to ensure meaningful progression of the polycondensation. Under these adjusted conditions, distinct trends in monomer conversion and structural development were observed. The experimental data obtained were analysed using the same modelling approach described for DVA, the contour plots were used to interpret the combined effects of the experimental factors on the measured responses in the AA system. Extended coefficient models and tables are provided in the Supporting Information – Section 3, Fig. S10 to Fig. S15 and Table S9 to Table S14.

The contour plots for conversion (%) of AA (Fig. 5) showed that conversion values ranged from 0 % to 96 % (determined by ^{1}H NMR, Supporting Information – Fig. S2B, Equation S2), revealing a pronounced dependence on reaction duration across all solvent systems. At shorter reaction times (6 h), conversion remains low in most media,

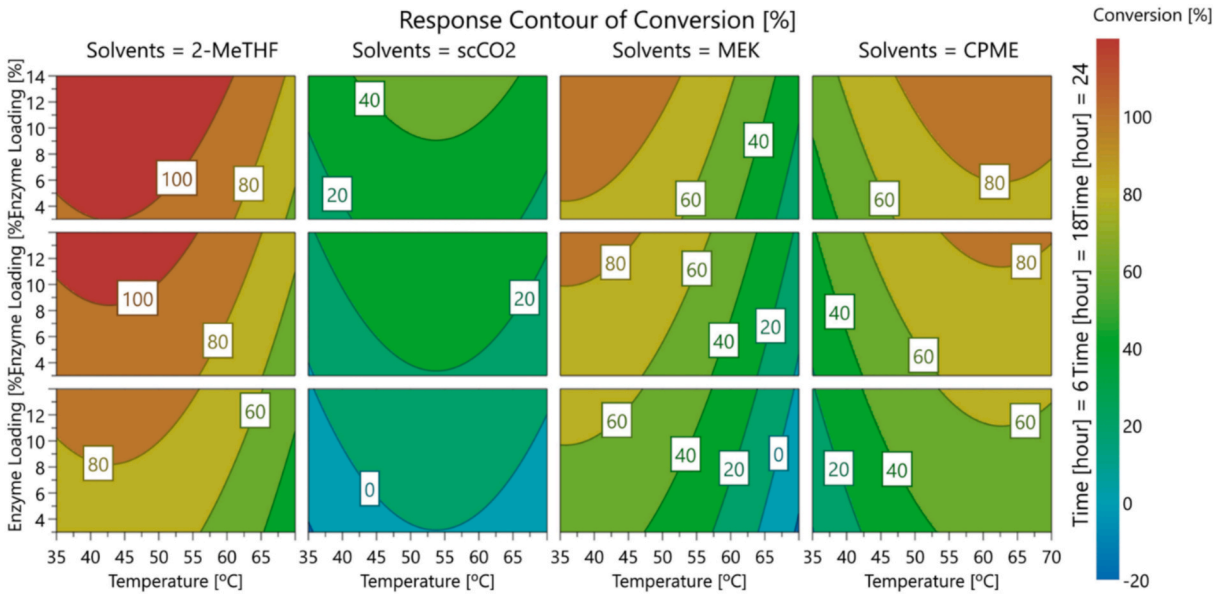

Fig. 5. Predicted conversion (%) contour plots for the AA reactions as a function of temperature and enzyme loading, presented for four solvents (2-MeTHF, $scCO_2$, MEK and CPME) at different reaction times (3, 5 and 7 h).

whereas extended reaction times (18–24 h) are required to achieve substantial monomer consumption. Among the solvents evaluated, 2-MeTHF enables near-quantitative conversion over a broad range of temperatures and enzyme loadings at 24 h. MEK and CPME exhibit intermediate behaviour, reaching moderate to high conversions under intensified conditions, particularly at elevated temperature and enzyme loading. In contrast, $scCO_2$ consistently yields limited conversion throughout the investigated domain, even at prolonged reaction times, indicating restricted progression of the reaction.

Higher temperatures promote increased conversion in CPME, whereas in 2-MeTHF and MEK elevated temperatures do not necessarily lead to higher conversion values. This behaviour may be associated with solvent-dependent solubility effects in CPME involving both monomers and the growing polymer chains. In CPME, increased temperatures are likely to enhance mass transfer and monomer availability, thereby facilitating conversion. A similar temperature-dependent limitation is observed in $scCO_2$, although overall conversion levels remain comparatively low in this medium. These differences in reaction progression directly influence the development of polymer microstructure, as reflected in the substitution patterns observed across the experimental domain. Similar solvent dependent effects on monomer conversion have been previously demonstrated by Farmer's group [46].

The contour plots for the 1,2,3-T response (Fig. 6A) indicate a pronounced dependence on reaction time, particularly in 2-MeTHF, MEK and CPME. At 6 h, 1,2,3-T levels remain modest across most solvents, whereas extended reaction times (18–24 h) promote a substantial increase in 1,2,3-T formation, particularly under elevated enzyme loading. Among the evaluated solvents, 2-MeTHF and CPME exhibit the highest predicted 1,2,3-T values at 24 h, while MEK displays intermediate behaviour. In contrast, $sccO_2$ shows consistently lower levels, in agreement with its limited conversion profile.

Meanwhile, the contour plots for 1,2-D (Fig. 6B) reveal solvent-dependent behaviour in the AA system. In 2-MeTHF and MEK, 1,2-D levels increase with reaction time, with higher values generally observed at extended reaction times. In these media, temperature also influences 1,2-D, with slightly higher levels appearing toward the lower temperature range. In contrast, CPME exhibits an opposite thermal trend, where increased temperature favours higher 1,2-D formation. For

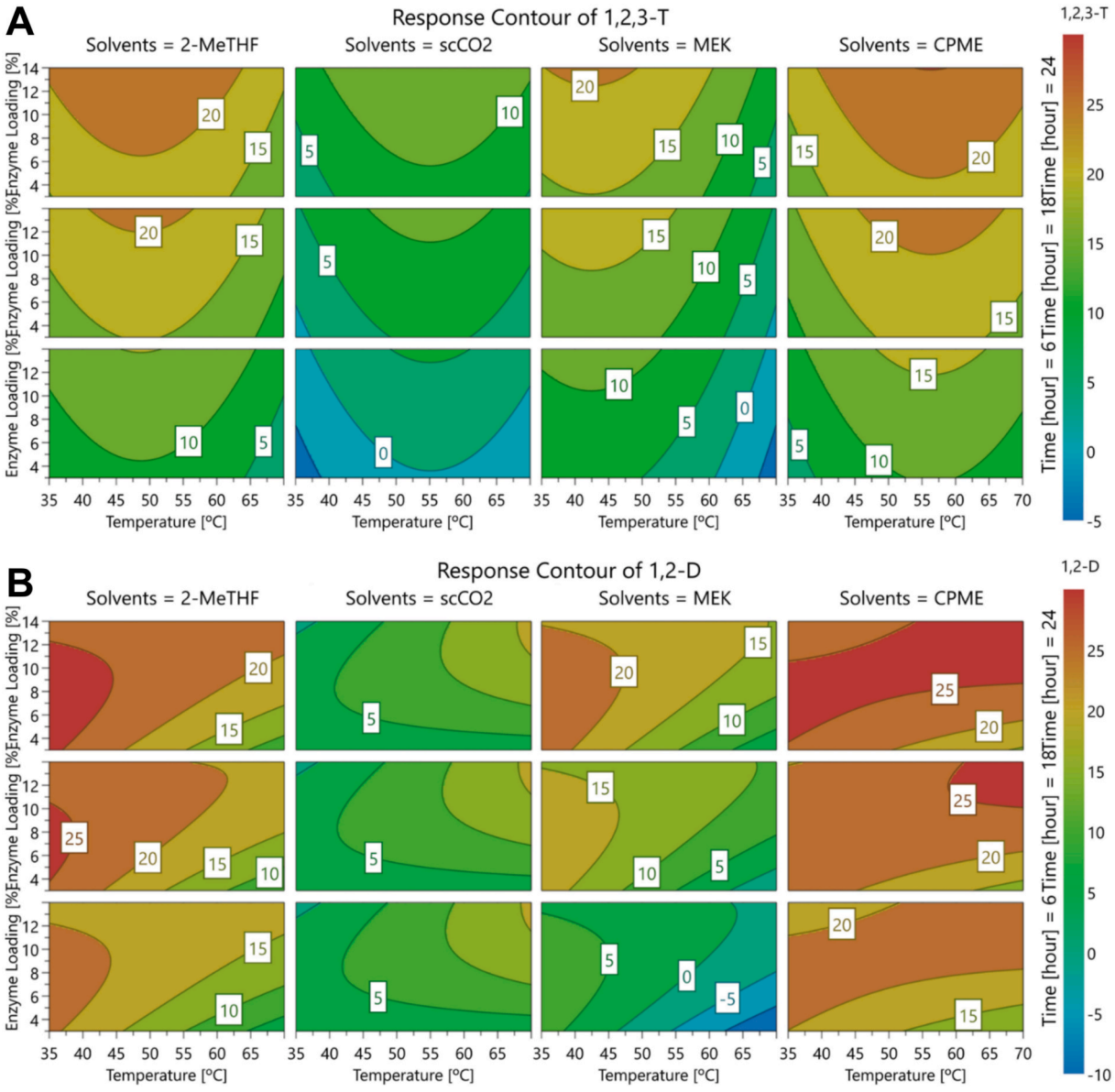

Fig. 6. Predicted (A) 1,2,3-Trisubstitution (%) and (B) 1,2-Disubstitution (%) contour plots for AA reactions as a function of temperature and enzyme loading, presented for four solvents (2-MeTHF, $scCO_2$, MEK and CPME) at different reaction times (3, 5 and 7 h).

$scCO_2$, the response surface remains largely flat across the investigated time range, with minimal variation in 1,2-D levels, consistent with the limited overall reaction progression observed in this medium.

The observed dependence of substitution patterns on reaction progression suggests that chain extension in the AA system is likewise strongly influenced by reaction time and catalytic availability. Since the formation of higher degrees of substitution reflects continued ester bond formation, the development of high-molecular-weight species is expected to correlate with conditions that enable sustained reaction advancement. In this context, analysis of the M_w provides insight into how effectively each solvent system supports the chain to grow beyond initial esterification events.

The contour plots for M_w (Fig. 7) reveal a strong dependence on reaction time and reaction temperature in the AA system with M_w values varying substantially over the reaction conditions screened, ranging from 260 to 36700 g/mol. At 6 h, M_w values remain below 10000 g/mol across all solvent systems, whereas extended reaction times enable the development of substantially higher molar mass fractions. It should be noted that the colour scale is largely influenced by the elevated M_w values obtained in 2-MeTHF at 24 h, which shifts the upper contour range and visually compresses differences in the lower molar mass regions. At 24 h, 2-MeTHF provides the highest predicted M_w values, exceeding 30000 g/mol under elevated enzyme loading. CPME and MEK exhibit intermediate behaviour, reaching moderate to high M_w values under harsh conditions, while $scCO_2$ shows consistently low molar masses across the investigated domain (280 g/mol to 1100 g/mol, Table S2), reflecting the poor conversion observed, which is associated with solubility and mass transfer limitations.

These results indicate that sustained reaction progression is required to achieve the highest molar mass fractions in the AA system. Moreover, solvent-specific differences remain evident in M_w development. In particular, $scCO_2$ exhibits a largely monotonic and uniformly low response surface, consistent with its limited conversion and, consequently, restricted polymer chain extension under the investigated conditions. Analysis of the number-average molar mass (M_n) is provided in the Supplementary Information – Section 3, Fig. S16. Notably, as was observed for DVA, high conversion did not always correspond to maximum M_w, indicating that chain extension depends not only on monomer consumption but also on solvent and catalytic conditions.

Beyond the extent of polymerisation, it is also important to evaluate how reaction conditions influence the distribution of molar masses. Analysis of $Đ$ therefore provides complementary insight into whether conditions leading to higher M_w are accompanied by broader molar mass distributions in the AA system. The contour plots for $Đ$ (Fig. 8) reveal a clear dependence on reaction time in the AA system. At 6 h, dispersity values remain low across all solvents, generally between 1 and 2, indicating relatively narrow molar mass distributions at early stages of the reaction. As reaction time increases to 18 and 24 h, $Đ$ progressively increases, particularly in 2-MeTHF, where values above 6 are observed under elevated enzyme loading. MEK and CPME exhibit intermediate behaviour, reaching moderate $Đ$ values under intensified conditions, whereas $scCO_2$ maintains comparatively low and monotonic $Đ$ profiles throughout the investigated domain. These results indicate that extended reaction progression not only promotes higher M_w but also leads to broader molar mass distributions, which is in consistent with the behaviour observed for DVA, since for the AA the 1,2,3-T values are also qualitatively correlated with the M_w, reflecting the same trend.

In general, solvent identity modulates the maximum attainable conversion and molar mass, with 2-MeTHF and CPME supporting more effective chain extension, while $scCO_2$ remains limited across all responses. In addition to the solvent effect, the responses for the AA experimental design space are strongly influenced by the extent of reaction, reflecting the differences in the intrinsic reactivity between the two adipate derivatives used in this study.

3.3. Solvent selection

Comparison between the two acyl counterparts highlights clear differences in reaction behaviour and process sensitivity. The DVA system achieves high conversion and substantial molar mass development over a broader experimental domain, whereas the AA system requires extended reaction times and higher catalytic availability to reach comparable levels of chain length. In the DVA system, solvent identity plays a dominant role in modulating both substitution patterns and molar mass development, while in the AA system, reaction progression emerges as the primary governing factor across all responses.

These trends reflect the intrinsic reactivity of the acyl counterparts. DVA undergoes lipase-catalysed transesterification in which the vinyl alcohol by-product rapidly tautomerizes to acetaldehyde, shifting the equilibrium toward polymer formation. In contrast, AA reacts through direct esterification, generating water that must be continuously removed to sustain polycondensation. Consequently, the AA system

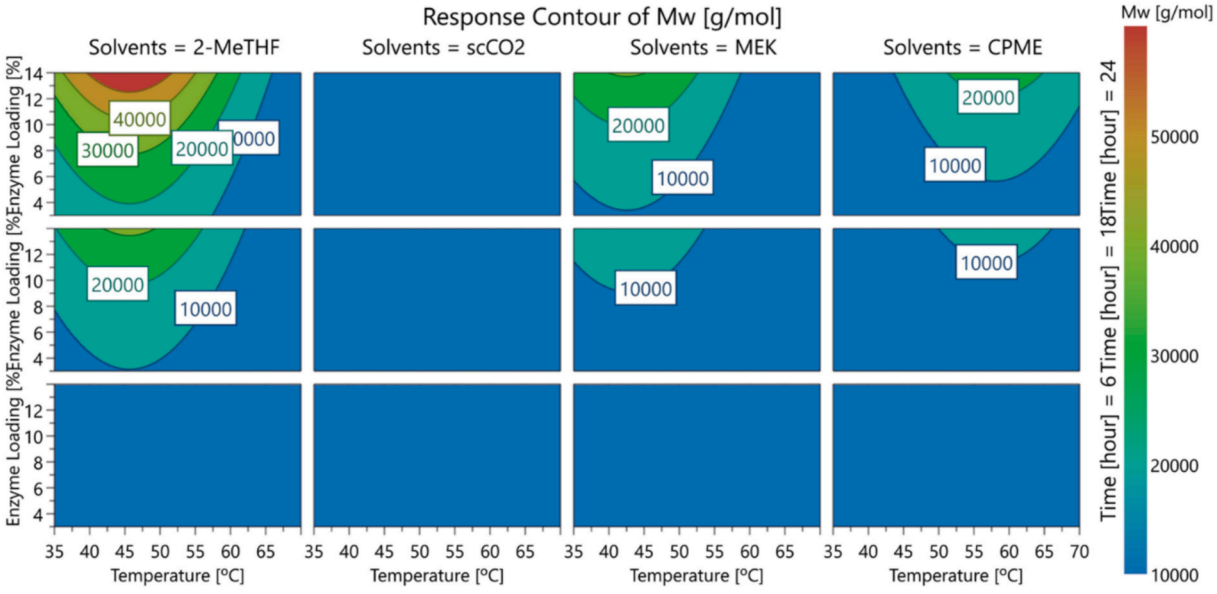

Fig. 7. Predicted M_w (g/mol) contour plots for AA reactions as a function of temperature and enzyme loading, presented for four solvents (2-MeTHF, $scCO_2$, MEK and CPME) at different reaction times (3, 5 and 7 h).

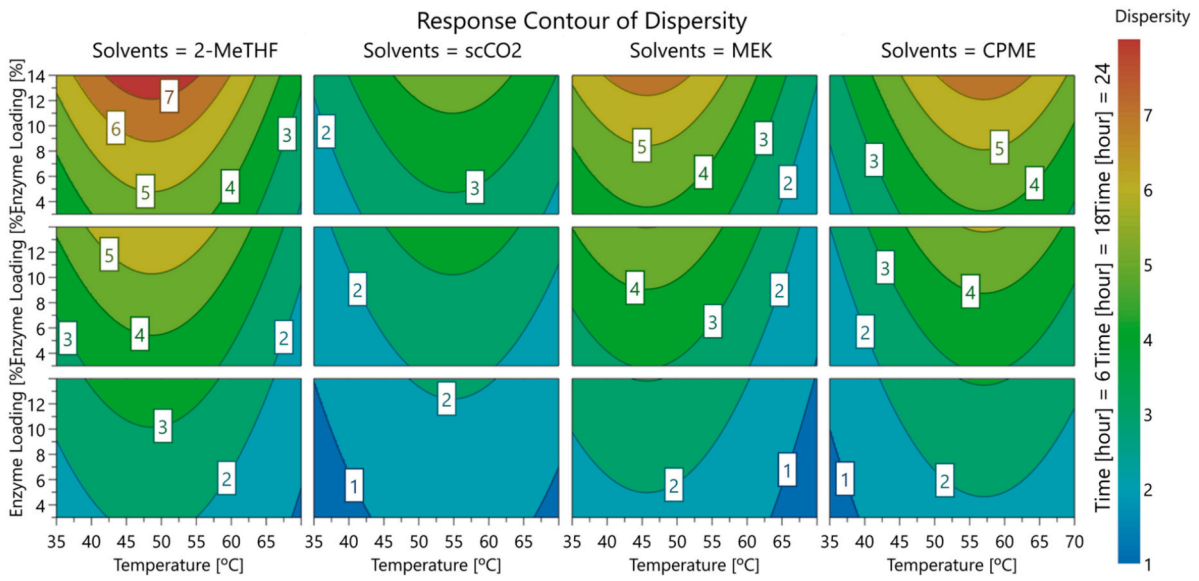

Fig. 8. Predicted Dispersity ($Đ$) contour plots for AA reactions as a function of temperature and enzyme loading, presented for four solvents (2-MeTHF, $scCO_2$, MEK and CPME) at different reaction times (3, 5 and 7 h).

shows a stronger dependence on reaction time and catalyst loading.

The DoE framework used enabled a systematic evaluation of solvent effects across the investigated reaction environments. Predicted contour plots identified solvent-dependent performance windows for each monomer system, revealing a broad range of responses across the experimental domain. Within this context, solvent identity played a central role in polymer growth. While 2-MeTHF consistently supports efficient polymerisation across both monomer systems, MEK and CPME displayed intermediate behaviour depending on the reaction regime. MEK, with a logP of 0.3, [47] generally enabled efficient monomer consumption but yields more moderate molar mass development, indicating that a more hydrophilic solvent is advantageous in this instance. CPME exhibited stronger sensitivity to temperature and enzyme loading, suggesting solubility limitations. Of the solvents investigated, CPME has the highest logP (1.3), suggesting that more hydrophobic solvents are not well suited to this reaction [48]. In contrast, $scCO_2$ restricts polymer formation in both systems, although this limitation is more pronounced for AA than for DVA, likely due to the limited solubility of the polar substrates and growing polymer chains, which reduces effective mass transfer and enzyme-substrate interactions. Despite the observed trend between logP and monomer conversion, complex enzyme-solvent interactions should also be considered in future work as it is likely that there are more intricate relationships and interactions to consider in this reaction.

Nevertheless, the interpretation of the response maps can be guided by the intended application as the optimal combination of parameters depends on the targeted outcomes, whether maximizing molar mass, controlling branching density, or tuning substitution patterns. These structural features, in turn, influence the suitability of the materials for subsequent applications, e.g., nanoparticle formulation. In this sense, the DoE approach does not merely optimize reaction conditions; it delineates how monomer reactivity, solvent properties, and processing variables collectively define the accessible materials space for specific applications.

4. Conclusions

This work demonstrates the effectiveness of a DoE strategy for systematically investigating the enzymatic synthesis of PGA in complex multifunctional systems. By simultaneously evaluating solvent, temperature, enzyme loading, and reaction time, the multivariate framework enabled a comprehensive exploration of the reaction space governing PGA formation. Across the investigated design domain, the experimental dataset revealed a broad and diverse response space, with distinct and solvent-dependent trends emerging for each monomer system.

For the transesterification system using DVA, monomer conversion spanned a wide range from 9 % to quantitative values, highlighting the strong sensitivity of the reaction to the surrounding solvent environment and catalytic conditions. High conversions were frequently achieved in 2-MeTHF and MEK across a broad range of temperatures and enzyme loadings, whereas CPME and $scCO_2$ required more intensified conditions to reach comparable monomer consumption. The resulting molar masses varied significantly across the design space, ranging from approximately 200 to 16300 g/mol, confirming that high conversion alone does not necessarily translate into extensive polymerisation.

In contrast, the esterification system employing AA displayed a narrower operational window and a stronger dependence on reaction progression. Conversion values ranged from 0 % to approximately 96 %, with substantial monomer consumption only achieved under extended reaction times and higher enzyme loadings. Under these conditions, molar masses between 260 and 36700 g/mol were obtained, demonstrating that prolonged reaction progression enables the formation of higher molar mass fractions in the AA system. These results highlight the fundamental differences in reactivity between DVA and AA, reflecting the distinct thermodynamic and kinetic characteristics of transesterification and direct esterification pathways.

Beyond overall conversion and molar mass development, the DoE analysis revealed systematic relationships between process variables and polymer microstructure. Increased temperature and enzyme loading generally promoted higher levels of glycerol substitution, while solvent identity modulated the balance between chain growing and structural complexity. In particular, 2-MeTHF consistently supported efficient polymer formation across both monomer systems, whereas $scCO_2$ displayed limited polymer growth under the investigated conditions, likely due to solubility and mass-transfer constraints. MEK and CPME exhibited intermediate behaviour, providing moderate to high conversions depending on the reaction regime.

The DoE methodology proved particularly valuable not only for reducing the number of experiments required but also for enabling the mathematical modelling of different solvents and their effects across the reaction space. This statistical framework allowed the construction of a

predictive and sustainable experimental space in which alternative reaction media can be systematically evaluated. Within this context, MEK, CPME and $scCO_2$ were investigated for the first time as solvents for enzymatic PGA synthesis, demonstrating how DoE screening can facilitate the exploration of greener solvent systems while keeping good catalytic performance.

Throughout the screenings, the concentration of monomers in solvent remained constant, except for the $scCO_2$ reactions. The concentration used in this study agrees with published literature, and positions our study well in the broader context of comparable systems. The chosen concentration facilitates good mass transfer, as is required for heterogeneous catalysis. Where monomers were not fully soluble in the reaction medium, as was observed with some of the solvents screened, mass transfer limited conversion. Variations in the concentration may result in changes in viscosity and mass transfer, as well as influencing the extent of intermolecular transesterification. Further probing of the reaction over a range concentrations would enable a more in-depth understanding of the effect of concentration on conversion, molar mass, and the polymer microstructure.

This work establishes enzymatic PGA synthesis as a versatile platform for understanding structure-process-property relationships in multifunctional polyester systems. The insights obtained here demonstrate how statistical experimental design can guide the rational selection of sustainable solvents and reaction conditions while enabling precise control over polymer architecture, ultimately supporting the development of greener and more tuneable polyester materials.

The authors declare that they have no known competing financial interests or personal relationships that could have appeared to influence the work reported in this article.

CRediT authorship contribution statement

Gabriel F.S. Brito: Writing – original draft, Visualization, Validation, Methodology, Investigation, Formal analysis, Data curation. **Emily G. Dixon:** Writing – review & editing, Validation, Software, Investigation, Data curation, Conceptualization. **Mei Y. Young:** Writing – review & editing, Validation, Supervision, Methodology, Formal analysis. **Adam Lee:** Writing – review & editing, Validation, Methodology. **Daniel M. Day:** Writing – review & editing, Visualization, Validation, Funding acquisition. **Amy R. Goddard:** Writing – review & editing, Validation, Supervision, Funding acquisition. **Fabricio Machado:** Writing – review & editing, Writing – original draft, Validation, Supervision, Software, Methodology, Funding acquisition. **Philippa L. Jacob:** Writing – review & editing, Visualization, Validation, Supervision, Resources, Project administration, Methodology, Investigation, Funding acquisition, Formal analysis, Data curation, Conceptualization. **Vincenzo Taresco:** Writing – review & editing, Writing – original draft, Validation, Supervision, Software, Resources, Project administration, Investigation, Funding acquisition, Conceptualization.

Declaration of competing interest

The authors declare that they have no known competing financial interests or personal relationships that could have appeared to influence the work reported in this paper.

Acknowledgements

GB acknowledges the Coordenação de Aperfeiçoamento de Pessoal de Nível Superior - Brasil (CAPES) - Finance Code 001. E.G.D. acknowledges the EPSRC/SFI CDT in Sustainable Chemistry— Atoms 2 Products (EP/S022236/1) for their funding support.

PLJ, ARG, AL, DMD and VT thank EPSRC for funding through Prosperity Partnership EP/X025489/1 undertaken in collaboration with Croda. PLJ was also supported by an EPSRC Doctoral Prize Fellowship [EP/W524402/1].

Appendix A. Supplementary data

Supplementary data to this article can be found online at https://doi.org/10.1016/j.eurpolymj.2026.114886.

Data availability

Data will be made available on request.

References

[1] Y. Zhu, C. Romain, C.K. Williams, Sustainable polymers from renewable resources, Nature 540 (7633) (2016) 354–362.
[2] J.G. Rosenboom, R. Langer, G. Traverso, Bioplastics for a circular economy, Nat. Rev. Mater. 7 (2) (2022) 117–137.
[3] C.T. Roberts, M.A. Grunlan, Biodegradable Polyesters: Approaches to increase Degradation rates for Biomedical applications, ACS Macro Lett. 14 (8) (2025) 1221–1240.
[4] C. Jerome, P. Lecomte, Recent advances in the synthesis of aliphatic polyesters by ring-opening polymerization, Adv. Drug Deliv. Rev. 60 (9) (2008) 1056–1076.
[5] Z. Guan, J. Zhang, W. Zhou, Y. Zhu, Z. Liu, Y. Zhang, Y. Zhang, Mechanistic details of the Titanium-Mediated Polycondensation Reaction of Polyesters: a DFT Study, Catalysts 13 (10) (2023).
[6] T. Zhang, B.A. Howell, A. Dumitrascu, S.J. Martin, P.B. Smith, Synthesis and characterization of glycerol-adipic acid hyperbranched polyesters, Polymer 55 (20) (2014) 5065–5072.
[7] S. Kobayashi, Enzymatic polymerization: a new method of polymer synthesis, J. Polym. Sci. A Polym. Chem. 37 (16) (1999) 3041–3056.
[8] R.A. Gross, M. Ganesh, W. Lu, Enzyme-catalysis breathes new life into polyester condensation polymerizations, Trends Biotechnol. 28 (8) (2010) 435–443.
[9] V. Hevilla, A. Sonseca, C. Echeverria, A. Munoz-Bonilla, M. Fernandez-Garcia, Enzymatic Synthesis of Polyesters and their Bioapplications: recent advances and Perspectives, Macromol. Biosci. 21 (10) (2021) e2100156.
[10] L.E. Iglesias, Y. Fukuyama, H. Nonami, R. Erra-Balsells, A. Baldessari, A simple enzymatic procedure for the synthesis of a hydroxylated polyester from glycerol and adipic acid, Biotechnol. Tech. 13 (12) (1999) 923–926.
[11] V. Taresco, R.G. Creasey, J. Kennon, G. Mantovani, C. Alexander, J.C. Burley, M. C. Garnett, Variation in structure and properties of poly(glycerol adipate) via control of chain branching during enzymatic synthesis, Polymer 89 (2016) 41–49.
[12] P. Kallinteri, S. Higgins, G.A. Hutcheon, C.B. St, M.C.G. Pourçain, Novel Functionalized Biodegradable Polymers for Nanoparticle Drug delivery Systems, Biomacromolecules 6 (4) (2005) 1885–1894.
[13] S.M.E. Swainson, I.D. Styliari, V. Taresco, M.C. Garnett, Poly (glycerol adipate) (PGA), an Enzymatically Synthesized Functionalizable Polyester and Versatile Drug delivery Carrier: a Literature Update, Polymers (basel) 11 (10) (2019).
[14] L. Navarro, N. Ceaglio, I. Rintoul, Structure and properties of biocompatible poly (glycerol adipate) elastomers modified with ethylene glycol, Polym. J. 49 (8) (2017) 625–632.
[15] P.L. Jacob, L.A. Ruiz Cantu, A.K. Pearce, Y. He, J.C. Lentz, J.C. Moore, F. Machado, G. Rivers, E. Apebende, M.R. Fernandez, I. Francolini, R. Wildman, S.M. Howdle, V. Taresco, Poly (glycerol adipate). (PGA) Backbone Modifications with a Library of Functional Diols: Chemical and Physical Effects, Polymer 228, 2021.
[16] V. Taresco, I. Tulini, I. Francolini, A. Piozzi, Polyglycerol Adipate-Grafted Polycaprolactone Nanoparticles as Carriers for the Antimicrobial compound Usnic Acid, Int. J. Mol. Sci. 23 (22) (2022).
[17] P.L. Jacob, B. Brugnoli, A. Del Giudice, H. Phan, V.M. Chauhan, L. Beckett, R. B. Gillis, C. Moloney, R.J. Cavanagh, E. Krumins, M. Reynolds-Green, J.C. Lentz, C. Conte, V. Cuzzucoli Crucitti, B. Couturaud, L. Galantini, I. Francolini, S. M. Howdle, V. Taresco, Poly (diglycerol adipate) variants as enhanced nanocarrier replacements in drug delivery applications, J. Colloid Interface Sci. 641 (2023) 1043–1057.
[18] E. Krumins, J.C. Lentz, B. Sutcliffe, A. Sohaib, P.L. Jacob, B. Brugnoli, V. Cuzzucoli Crucitti, R. Cavanagh, R. Owen, C. Moloney, L. Ruiz-Cantu, I. Francolini, S. M. Howdle, M. Shusteff, F. Rose, R.D. Wildman, Y. He, V. Taresco, Glycerol-based sustainably sourced resin for volumetric printing, Green Chem. 26 (3) (2024) 1345–1355.
[19] H. Kricheldorf, Paul J. Flory and the Classical Theory of Polycondensation, in: H. Kricheldorf (Ed.), Polycondensation: History and New Results, Springer, Berlin Heidelberg, Berlin, Heidelberg, 2014, pp. 35–50.
[20] Y. Wang, G.A. Ameer, B.J. Sheppard, R. Langer, Y. Wang, G.A. Ameer, B. J. Sheppard, R. Langer, A tough biodegradable elastomer, Nat. Biotechnol. 20 (20) (2002) 602–606.
[21] S. Andrä-Żmuda, P. Chaber, M.M. Maksymiak, M. Musioł, G. Adamus, Poly (glycerol sebacate): A Comparative Study of Various Synthesis Methods, Biomacromolecules 26(11) (October 4, 2025).
[22] T. Naolou, V.M. Weiss, D. Conrad, K. Busse, K. Mäder, J. Kressler, Fatty Acid Modified Poly(glycerol adipate) - Polymeric Analogues of Glycerides, Tailored Polymer Architectures for Pharmaceutical and Biomedical Applications (2013) 39–52.
[23] G.B. Perin, M.I. Felisberti, Polyesters inspired by Glycerides: Enzymatic Polycondensation, Structure, Properties, and Nanoparticle Preparation, Macromolecules 56 (17) (2023) 6968–6977.

[24] E.G. Dixon, E. Chau, L. Ciano, A. Pordea, K. Alvey, V. Taresco, D-Optimal Design for Enzymatic Ring-Opening Polymerization of ε-Caprolactone: Toward Sustainable Polyester Synthesis using Biobased Solvents, J. Polym. Sci. 64 (3) (2026) 817–824.
[25] F. Fabbri, F.A. Bertolini, G.M. Guebitz, A. Pellis, Biocatalyzed Synthesis of Flavor Esters and Polyesters: a Design of Experiments (DoE) Approach, Int. J. Mol. Sci. 22 (16) (2021).
[26] A.E. Polloni, J.G. Veneral, E.A. Rebelatto, D. de Oliveira, J.V. Oliveira, P.H. H. Araújo, C. Sayer, Enzymatic ring opening polymerization of ω-pentadecalactone using supercritical carbon dioxide, J. Supercrit. Fluids 119 (2017) 221–228.
[27] C. Guindani, W.A.G. Jaramillo, G. Candiotto, E.A. Rebelatto, F.W. Tavares, J. C. Pinto, P.M. Ndiaye, M. Nele, Synthesis of polyglobalide by enzymatic ring opening polymerization using pressurized fluids, J. Supercrit. Fluids 186 (2022).
[28] R.D. Santos, E.A. Rebelatto, C. Guindani, H.B. Madalosso, L. Scorsin, D.A. Mayer, J. V. Oliveira, Lipase-catalyzed synthesis of poly(ω-pentadecalactone-co-globalide) in supercritical carbon dioxide, J. Supercrit. Fluids 215 (2025).
[29] S.R. Rosso Comim, J.G. Veneral, D. de Oliveira, S.R.S. Ferreira, J.V. Oliveira, Enzymatic synthesis of poly(ε-caprolactone) in liquified petroleum gas and carbon dioxide, J. Supercrit. Fluids 96 (2015) 334–348.
[30] R.D. Santos, S.R. Rosso Comim, D.d. Oliveira, H. Treichel, M. Di Luccio, S.R.S. Ferreira, J. Vladimir Oliveira, Lipase-catalyzed synthesis of poly(e-caprolactone) in supercritical carbon dioxide, Biocatal. Agric. Biotechnol. 1 (4) (2012) 280–283.
[31] A. Pellis, J.W. Comerford, A.J. Maneffa, M.H. Sipponen, J.H. Clark, T.J. Farmer, Elucidating enzymatic polymerisations: Chain-length selectivity of Candida antarctica lipase B towards various aliphatic diols and dicarboxylic acid diesters, Eur. Polym. J. 106 (2018) 79–84.
[32] G.B. Perin, M.I. Felisberti, Enzymatic Synthesis of Poly(glycerol sebacate): Kinetics, Chain Growth, and Branching Behavior, Macromolecules 53 (18) (2020) 7925–7935.
[33] K.M. Saller, L. Graf, A. Kruglhuber, C. Schwarzinger, Acidity and polarity – Overcoming challenges of the enzyme catalyzed polycondensation of adipic acid and 1,4-butanediol, Polymer 327 (2025) 128419.
[34] H.H. Khoo, L.L. Wong, J. Tan, V. Isoni, P. Sharratt, Synthesis of 2-methyl tetrahydrofuran from various lignocellulosic feedstocks: Sustainability assessment via LCA, Resour. Conserv. Recycl. 95 (2015) 174–182.
[35] E. Sánchez-Ramírez, S. Hernández, A.G. Romero-García, H. Alcocer-García, J.G. Segovia – Hernández, Synthesis and Optimization of Sustainable Processes Based on Liquid-Liquid Extraction to Purify Methyl Ethyl Ketone, Chemical Engineering and Processing - Process Intensification 171 (2022).
[36] D. Prat, A. Wells, J. Hayler, H. Sneddon, C.R. McElroy, S. Abou-Shehada, P.J. Dunn, CHEM21 selection guide of classical- and less classical-solvents, Green Chem. 18 (1) (2016) 288–296.
[37] V. Hessel, N.N. Tran, M.R. Asrami, Q.D. Tran, N. Van Duc Long, M. Escribà-Gelonch, J.O. Tejada, S. Linke, K. Sundmacher, Sustainability of green solvents – review and perspective, Green Chem. 24 (2) (2022) 410–437.
[38] K. Watanabe, N. Yamagiwa, Y. Torisawa, Cyclopentyl Methyl Ether as a New and Alternative Process Solvent, Org. Process Res. Dev. 11 (2) (2007) 251–258.
[39] C.A. Curie, M.A. Darmawan, D. Dianursanti, W. Budhijanto, M. Gozan, The effect of Solvent Hydrophilicity on the Enzymatic Ring-opening Polymerization of L-Lactide by Candida rugosa Lipase, Polymers (basel) 14 (18) (2022) 3856.
[40] A.E.M. Janssen, M. Hadini, N. Wessels Boer, R. Walinga, A. Van der Padt, H.M. Van Sonsbeek, K. Van't Riet, in: The Effect of Organic Solvents on Enzymatic Esterification of Polyols, Progress in Biotechnology, Elsevier 1992,, pp. 155–161.
[41] G. Englezou, K. Kortsen, A.A.C. Pacheco, R. Cavanagh, J.C. Lentz, E. Krumins, C. Sanders-Velez, S.M. Howdle, A.J. Nedoma, V. Taresco, 2-Methyltetrahydrofuran (2-MeTHF) as a versatile green solvent for the synthesis of amphiphilic copolymers via ROP, FRP, and RAFT Tandem Polymerizations, Journal of Polymer Science 58 (11) (2020) 1571–1581.
[42] P.G. Jessop, Searching for green solvents, Green Chem. 13 (6) (2011) 1391–1398.
[43] D. Prat, J. Hayler, A. Wells, A survey of solvent selection guides, Green Chem. 16 (10) (2014) 4546–4551.
[44] M. Takwa, Y. Xiao, N. Simpson, E. Malmström, K. Hult, C.E. Koning, A. Heise, M. Martinelle, Lipase Catalyzed HEMA Initiated Ring-opening Polymerization, In Situ Formation of Mixed Polyester Methacrylates by Transesterification, Biomacromolecules 9 (2) (2008) 704–710.
[45] M. D'Almeida Gameiro, A. Goddard, V. Taresco, S.M. Howdle, Enzymatic one-pot synthesis of renewable and biodegradable surfactants in supercritical carbon dioxide (scCO2), Green Chem. 22 (4) (2020) 1308–1318.
[46] T.F.C. Salum, D. Day, J. Sherwood, A. Pellis, T.J. Farmer, Enzymatic synthesis of aromatic biobased polymers in green, low-boiling solvents, J. Biotechnol. 396 (2024) 1–9.
[47] N.C.f.B. Information, PubChem Compound Summary for CID 6569, Methyl Ethyl Ketone, 2026. https://pubchem.ncbi.nlm.nih.gov/compound/methyl%20ethyl%20ketone. (Accessed 8th April 2026).
[48] N.C.f.B. Information, PubChem Compound Summary for CID 138539, Cyclopentyl methyl ether, 2026. https://pubchem.ncbi.nlm.nih.gov/compound/Cyclopentyl-methyl-ether. (Accessed 8th April 2026).